

# The Aquaporin 1 C-Terminal Tail Is Required for Migration and Growth of Pulmonary Arterial Myocytes

Ning Lai<sup>1,2</sup>, Julie Lade<sup>2</sup>, Kyle Leggett<sup>2</sup>, Xin Yun<sup>1,2</sup>, Syeda Baksh<sup>2</sup>, Eric Chau<sup>2</sup>, Michael T. Crow<sup>2</sup>, Venkataramana Sidhaye<sup>2</sup>, Jian Wang<sup>1,2</sup>, and Larissa A. Shimoda<sup>2</sup>

<sup>1</sup>Guangzhou Institute of Respiratory Diseases, State Key Laboratory of Respiratory Diseases, The First Affiliated Hospital, Guangzhou Medical University, Guangzhou, People's Republic of China; and <sup>2</sup>Division of Pulmonary and Critical Care Medicine, Department of Medicine, Johns Hopkins School of Medicine, Baltimore, Maryland

## Abstract

Pulmonary arterial smooth muscle cell (PASMC) proliferation and migration are important contributors to the vascular remodeling that occurs during development of pulmonary hypertension. We previously demonstrated that aquaporin (AQP)1, a member of the water channel family of proteins, was expressed in PASMCs and was necessary for hypoxia-induced migration; however, the mechanism by which AQP1 controls this response is unclear. The C-terminal tail of AQP1 contains putative calcium (EF-hand) and protein binding sites. Thus, we wanted to explore whether the C-terminal tail or the EF-hand motif of AQP1 was required for migration and proliferation. Rat PASMCs were isolated from distal pulmonary arteries, and proliferation and migration were measured using BrdU incorporation and transwell filters, respectively. To deplete AQP1, PASMCs were transfected with AQP1 small interference RNA (siRNA) or nontargeting siRNA. Knockdown of AQP1 reduced basal proliferation and hypoxia-induced migration and proliferation in PASMCs. In subsequent experiments, wild-type AQP1, AQP1 lacking the entire cytoplasmic C-terminal tail, or AQP1 with a mutation in the EF-hand motif were expressed in PASMCs using adenoviral

constructs. For all AQP1 constructs, infection increased AQP1 protein levels, water permeability, and the change in cell volume induced by hypotonic challenge. Infection with wild-type and EF-hand mutated AQP1, but not C-terminal-deleted AQP1, increased PASMC migration and proliferation. Our results suggest that AQP1 controls proliferation and migration in PASMCs and that the mechanism requires the C-terminal tail of the protein but is independent of water transport or the EF-hand motif.

**Keywords:** hypoxia; proliferation; EF-hand motif; smooth muscle cells

## Clinical Relevance

The study provides new information regarding the mechanisms controlling pulmonary arterial smooth muscle cell proliferation and migration, hallmark characteristics of pulmonary hypertension. The role of aquaporin 1 is attributed to the C-terminal tail rather than water transport, providing a novel mechanism for control of cell function.

Alveolar hypoxia, a consequence of many lung diseases, adversely affects the pulmonary vasculature. The changes that occur in the pulmonary circulation with exposure to chronic hypoxia include reductions in pulmonary arterial diameter due to contraction and structural remodeling of the vasculature, which result

in increased pulmonary vascular resistance and the development of pulmonary hypertension (1–3). The vascular remodeling that occurs in the lung is due, in part, to proliferation and migration of pulmonary arterial smooth muscle cells (PASMCs) (4). Although evidence of PASMC proliferation comes from studies

showing that medial hypertrophy in resistance-sized vessels was associated with an increased number of proliferating cell nuclear antigen-positive cells in rats or mice exposed to chronic hypoxia (5–7), migration of PASMCs is likely to be involved in the extension of smooth muscle down the vascular tree into small

(Received in original form August 28, 2013; accepted in final form November 25, 2013)

Correspondence and requests for reprints should be addressed to Larissa A. Shimoda, Ph.D., Division of Pulmonary and Critical Care Medicine, Johns Hopkins University, 5501 Hopkins Bayview Circle, 4A.52, Baltimore, MD 21224. E-mail: shimodal@welch.jhu.edu; or Ning Lai, M.D., Ph.D., Guangzhou Institute of Respiratory Diseases, State Key Laboratory of Respiratory Diseases, The First Affiliated Hospital, Guangzhou Medical University, 151 Yanjiang Road, Guangzhou, Guangdong, People's Republic of China. E-mail: congratulation2001@163.com

This article has an online supplement, which is accessible from this issue's table of contents at [www.atsjournals.org](http://www.atsjournals.org)

Am J Respir Cell Mol Biol Vol 50, Iss 6, pp 1010–1020, Jun 2014

Copyright © 2014 by the American Thoracic Society

Originally Published in Press as DOI: 10.1165/rcmb.2013-0374OC on December 11, 2013

Internet address: [www.atsjournals.org](http://www.atsjournals.org)

pulmonary vessels that are typically nonmuscular (1, 2, 8). Despite extensive study, the exact mechanisms underlying growth and migration of PSMCs and pulmonary vascular remodeling during the development of pulmonary hypertension remain incompletely understood.

Aquaporins (AQPs) are a family of small membrane-spanning proteins that transport water and in some cases small solutes such as glycerol. At least 13 mammalian AQPs have been confirmed to be expressed in a variety of cell types, including endothelial, epithelial, and smooth muscle cells (9–12). AQP1 was the first family member identified (13) and has since been shown to aid in the migration of epithelial, endothelial, smooth muscle, and tumor cells (10–12, 14–16); however, the mechanism by which AQP1 facilitates cellular migration remains unclear. We recently reported that AQP1, AQP4, and AQP7 are expressed in PSMCs, but only AQP1 is up-regulated by hypoxia (10). The up-regulation of AQP1 protein in response to hypoxia was dependent on  $\text{Ca}^{2+}$  influx and was required for hypoxia-induced PSMC migration (10). Whether AQP1 participates in regulating PSMC growth at baseline or in response to hypoxia has not been determined.

AQP1 is composed of six transmembrane  $\alpha$ -helices with cytoplasmic amino and carboxyl termini (17, 18). The 37-amino-acid C-terminal tail of AQP1 contains a putative EF-hand motif (19), a helix-loop-helix structural domain found in a large family of calcium-binding proteins. The EF-hand consists of two  $\alpha$  helices positioned roughly perpendicular to one another and linked by a short loop region that usually binds calcium ions. The role of this putative EF-hand domain in AQP1 is unknown.

Because our previous studies demonstrated a necessary role for AQP1 in mediating PSMC migration (10), in this study we further explored the role of AQP1 in regulating PSMC function by determining the effects of altering AQP1 levels, using silencing and expression techniques, on proliferation and migration in PSMCs. Moreover, because AQP1 contains potential protein binding sites and a putative calcium-binding site in its C-terminus, which might regulate AQP1 function, we hypothesized that the EF-hand motif in the C-terminal tail of AQP1 would

be required for migration and proliferation. To test this hypothesis, we evaluated the effect that loss of the putative EF-hand motif or the entire C-terminal tail of AQP1 had on PSMC migration and proliferation.

## Materials and Methods

All procedures were performed in accordance with the NIH Guide for the Care and Use of Laboratory Animals and were approved by the Johns Hopkins University Animal Care and Use Committee. A detailed description of all methods can be found in the online supplement.

### Isolation of PSMCs

PSMCs were isolated from adult, male Wistar rats as previously described (10). PSMCs were exposed to hypoxia *in vitro* by placing cells in an airtight chamber (Billups-Rothberg, Del Mar, CA) gassed with 4%  $\text{O}_2$ ; 5%  $\text{CO}_2$ . The nonhypoxic controls and chamber were placed in an incubator at 37°C for 24 hours for migration experiments or for 96 hours for proliferation experiments.

### AQP1 Constructs

Adenoviral constructs containing wild-type AQP1 (AdAQP1), a hemagglutinin (HA)-tagged wild-type AQP1 (AdAQP1-HA), AQP1 with C-terminal deletion (AdAQP1CT-HA), and AQP1 with an EF-hand mutation (AdAQP1M-HA) were created as described in the online supplement. PSMCs were infected with 50 infectious units per cell of virus before being used in functional assays and protein expression measurements.

### Migration Assays

Transwell migration assays were performed as previously described (10).

### Small Interference RNA Transfection

AQP1 depletion using small interference RNA (siRNA) was achieved as previously described (10).

### Proliferation Assays

Cell proliferation was determined using a commercially available kit for BrdU incorporation (GE HealthCare Life Sciences, Buckinghamshire, UK).

### Surface Biotinylation

PSMCs were washed, and a cell-impermeable biotin derivative was added to biotinylate surface proteins. Unreacted biotin was quenched and PSMCs lysed in solubilization buffer. Immunoprecipitation of biotinylated proteins was performed using equal amounts of total protein and streptavidin-linked agarose beads. Immunoprecipitates were washed in solubilization buffer, eluted, and subjected to immunoblotting with anti-AQP1.

### Immunofluorescence and Confocal Microscopy

PSMCs grown on glass slides were partially trypsinized to induce cell rounding, washed, fixed, and permeabilized. Cells were then blocked in goat serum, washed, and incubated with anti-AQP1 or anti-HA followed by incubation with fluorescent-conjugated secondary antibodies. Cell membranes were stained with membrane marker and observed with laser scanning confocal microscopy at 1- $\mu\text{m}$  step intervals over the entire z-axis.

### Estimation of Water Transport

To determine the water transport function of expressed constructs, two methods were used. First, we used a cell-swelling assay. Cells were trypsinized and replated onto glass coverslips for 1 hour, placed in a closed chamber, and perfused with HEPES-buffered solutions of varying osmotic pressure. Images of the cells were captured, cell diameters were measured using Image J software, and cell volume was calculated using the formula for sphere volume. Because the cells used in the swelling assay were only minimally attached to the coverslip, rapid transition of chamber fluid was not possible. Thus, water transport was also estimated using the calcein self-quenching method (20, 21). The decrease in calcein fluorescence with the change from hypotonic to hypertonic solution was fit with a single exponential, and the time constant calculated for each cell. Time constants ( $\tau$ ) for all cells within an experiment were averaged to obtain a single value per experiment.

### Statistical Analysis

A detailed description of the statistical analysis is provided in the online supplement.

## Results

### Effects of AQP1 Knockdown on PASMCMigration and Proliferation

To determine the role of AQP1 in PASMCMigration and proliferation, siRNA was used to reduce the levels of AQP1 expression. Efficacy of AQP1 reduction was

verified by immunoblot analysis (Figure 1A), which showed that exposure of PASMCMs to AQP1 siRNA (siAQP1) decreased AQP1 protein by an average of 70% compared with cells transfected with nontargeting siRNA (siNT). Next, we examined the effect of AQP1 knockdown on PASMCMigration and proliferation

under control (20% O<sub>2</sub>; 5% CO<sub>2</sub>) and hypoxic conditions (4% O<sub>2</sub>; 5% CO<sub>2</sub>). Compared with cells infected with siNT, treatment with siAQP1 had no effect on cell adherence (Figure 1B). PASMCMs treated with siNT and exposed to hypoxia exhibited significantly greater migration and proliferation than control PASMCMs

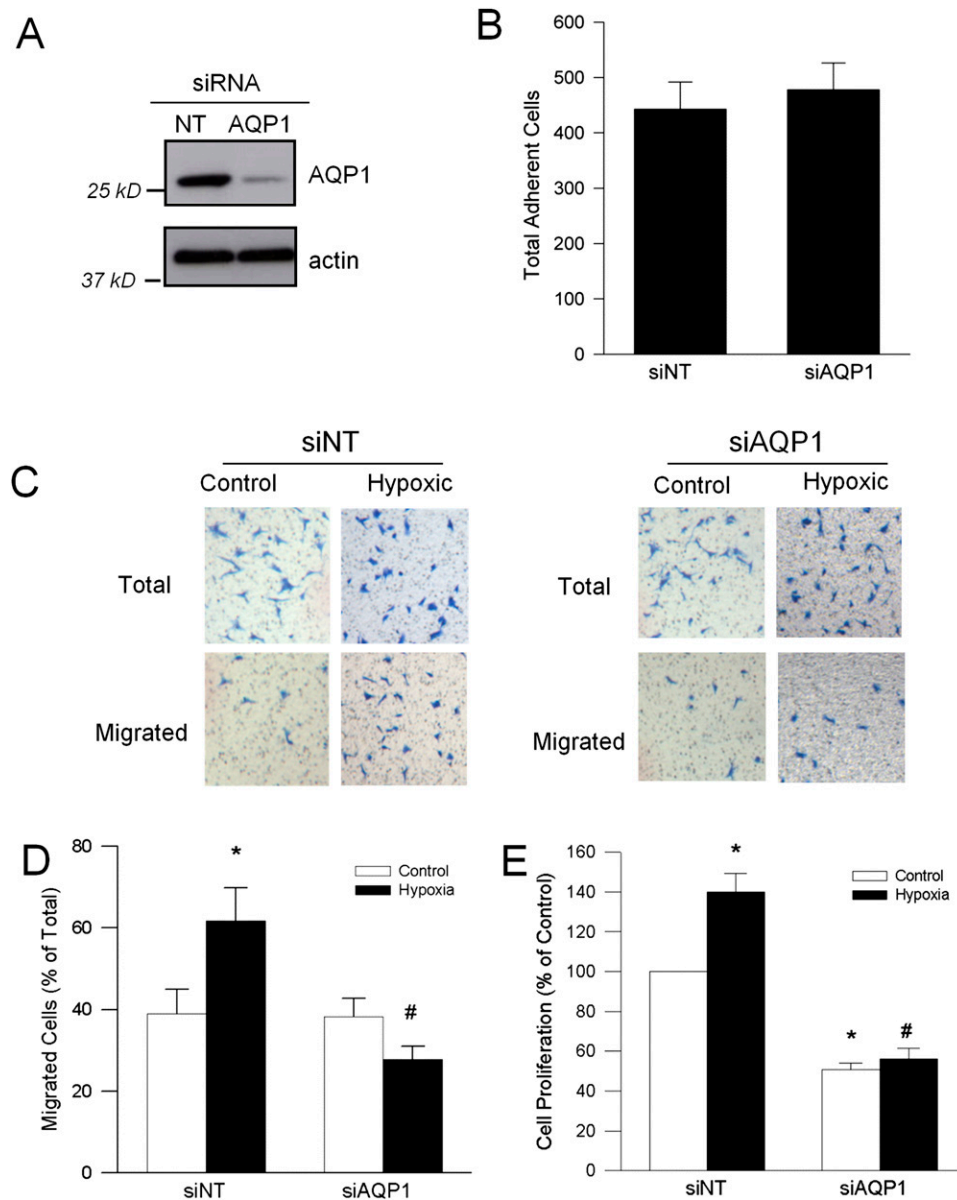


**Figure 1.** Effects of aquaporin 1 (AQP1) knockdown on pulmonary arterial smooth muscle cell (PASMCM) migration and proliferation. (A) Representative immunoblot images showing effects of small interference RNA (siRNA) directed against AQP1 (siAQP1) or nontargeting (NT) siRNA (siNT) on AQP1 and smooth muscle–specific  $\alpha$ -actin (actin) protein levels. (B) Bar graph showing mean  $\pm$  SEM values for cell adherence (total cells per membrane field) in cells treated with siNT or siAQP1 ( $n = 4$  each). (C) Representative images showing cells (stained with Brilliant Blue) before and after removal of unemigrated cells under different conditions. (D) Bar graph showing the percent migration (mean  $\pm$  SEM) in cells treated with siNT and siAQP1 under control (20% O<sub>2</sub>; 5% CO<sub>2</sub>) and hypoxic conditions (4% O<sub>2</sub>; 5% CO<sub>2</sub>) for 24 hours ( $n = 4$  for each group). (E) Bar graph shows proliferation (mean  $\pm$  SEM) in PASMCMs treated with siNT and siAQP1 under control (20% O<sub>2</sub>; 5% CO<sub>2</sub>) and hypoxic conditions (4% O<sub>2</sub>; 5% CO<sub>2</sub>) for 96 hours ( $n = 4$  for each group). \*Significant difference from control siNT ( $P < 0.05$ ). #Significant difference from hypoxic siNT ( $P < 0.05$ ).

(Figures 1C–1E). Under control conditions, treatment with siAQP1 had no significant effect on migration but significantly reduced the basal rate of proliferation. Treatment with siAQP1 completely prevented the hypoxia-induced increase in migration and proliferation.

### Effect of Increasing AQP1 Expression on PASC Migration and Proliferation

Because loss-of-function experiments suggested that AQP1 was involved in basal PASC proliferation and in the induction of proliferation and migration in response to hypoxia, we next tested whether increasing the expression of AQP1 in PASCs under nonhypoxic conditions would mimic the effect of hypoxia. Infection with AdAQP1 significantly increased total protein expression of AQP1 compared with cells infected with adenovirus-containing green fluorescent protein (AdGFP) (Figure 2A) approximately 3-fold, similar to levels observed with hypoxic exposure (10). To verify that the expressed AQP1 protein was trafficking properly, we used surface biotinylation to assess the amount of AQP1 inserted into the membrane and immunofluorescence to examine protein/membrane colocalization. Infection with AdAQP1 significantly increased surface biotinylation of AQP1 compared with the cells infected with AdGFP (Figure 2B). In immunofluorescence experiments, Z-stacks of cells infected with AdGFP show clear distinction between the membrane (Figure 2C, red) and GFP (Figure 2C, green), indicating cytosolic localization of GFP, as expected. In PASCs infected with AdAQP1, merged images show complete colocalization of AQP1 and the membrane. Compared with cells infected with AdGFP, treatment with AdAQP1 had no effect on cell adherence (total cell number =  $313 \pm 46$  cells for AdGFP vs.  $365 \pm 51$  cells for AdAQP1;  $n = 13$  and  $5$ , respectively) but significantly increased PASC migration and proliferation (Figures 2D and 2E) to levels similar to those observed with hypoxia.

### Cellular Localization of Mutant Constructs

To test whether the C-terminal tail or EF-hand motif in the tail of AQP1 was required for the effects of AQP1 on migration and proliferation, we generated

AdAQP1CT-HA and AdAQP1M-HA AQP1 constructs. Because the AQP1 antibody recognizes an epitope on the C-terminal, these proteins were created to express an HA-tag to allow visualization. We also generated AdAQP1-HA, which allowed us to compare protein levels of wild-type and mutated AQP1. Confocal microscopy was used to determine whether these constructs produced proteins that exhibited correct membrane localization (Figure 3A). In PASCs infected with AdAQP1-HA, AdAQP1CT-HA, and AdAQP1M-HA, merged images show complete colocalization between HA-tagged proteins and membrane stain, indicating that wild-type AQP1 with the HA-tag, AQP1 without the C-terminal, and AQP1 with EF-hand mutation correctly localize to the cell membrane.

### Volume Changes in Cells Expressing AQP1 Mutants

To establish the functionality of expressed AQP1 wild-type and mutant proteins, a cell-swelling assay was performed. Cell volume was first assessed under isotonic conditions, where no differences in initial cell volume were observed between groups. Cells expressing the appropriate constructs were perfused with hypertonic HEPES-buffered solution to induce maximum shrinkage, after which cells were exposed to hypotonic solution, and the change in volume was measured. PASCs infected with AdAQP1, AdAQP1CT-HA, or AdAQP1M-HA exhibited similar increases in cell volume in response to perfusion with hypotonic solution with respect to rate of change and maximum volume reached (Figures 3C–3E). In each case, infection with an AQP1 construct resulted in faster changes in volume (Figure 3D) and greater maximum volume reached (Figure 3E) compared with cells infected with AdGFP.

### Calcein Quenching in Cells Expressing AQP1 Mutants

To further characterize the water transport function of expressed AQP1 constructs, calcein self-quenching was used to estimate water flux across the membrane. Using methods previously described for adherent cells (20, 21), changes in calcein fluorescence were readily observed with rapid changes in perfusate (Figure 4A). The time constant ( $\tau$ ) for change in calcein quenching when perfusate was switched

from 140 to 380 mOsm was not different in untreated cells and cells expressing AdGFP (data not shown). Compared with GFP-expressing cells,  $\tau$  decreased by 32% in PASCs infected with wild-type AQP1 (Figure 4B), indicating faster water transport and cell volume change. Similar reductions in  $\tau$  were observed in cells infected with AdAQP1CT-HA or AdAQP1M-HA, confirming that the mutated constructs had similar water transport properties as the wild-type AQP1.

### Effects of C-Terminal Deletion on PASC Migration and Proliferation

We further confirmed that AQP1 with C-terminal deletion was adequately expressed and inserted into the membrane by measuring total protein via immunoblot and surface biotinylation (Figures 5A–5D). To determine whether addition of the HA-tag altered AQP1 protein expression, samples were first probed with an antibody against AQP1. PASCs infected with AdAQP1 or AdAQP1-HA expressed more total and membrane inserted AQP1 protein compared with cells infected with AdGFP, with native and HA-tagged AQP1 protein appearing as two separate bands (Figures 5A and 5B), indicating that addition of the HA-tag did not reduce AQP1 protein expression or membrane localization. Using anti-AQP1, only bands for native AQP1, similar to AdGFP, were detected for AdAQP1CT-HA (data not shown). However, as expected, bands for HA-tagged wild-type AQP1 and AQP1 with C-terminal deletion (slightly smaller size) were readily detected using anti-HA, which did not recognize native AQP1 proteins, as demonstrated by the lack of bands in AdGFP-infected cells and cells expressing untagged AQP1 (Figures 5C and 5D). Infection with AdAQP1CT-HA produced higher levels of total and membrane AQP1 protein than did expression of wild-type AQP1; even so, infection with AdAQP1CT-HA had no effect on PASC adherence ( $314 \pm 110$  cells [ $n = 5$ ] vs.  $313 \pm 46$  cells for AdGFP [ $n = 13$ ]), migration, or proliferation (Figures 5E and 5F) when compared with cells infected with AdGFP. These results are in contrast to the induction of migration and proliferation observed when wild-type AQP1 was expressed (Figures 2D and 2E).

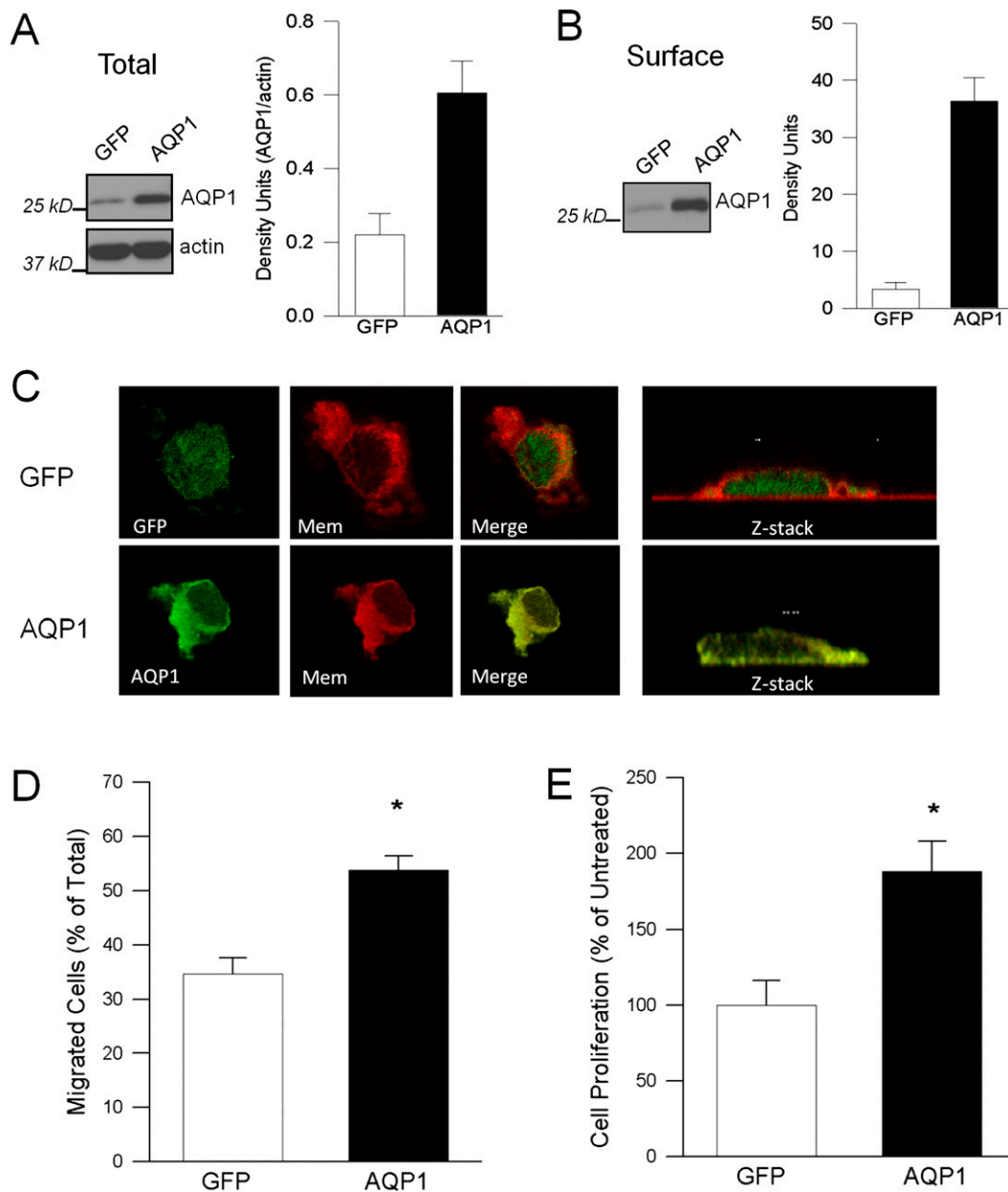


**Figure 2.** Effects of AQP1 overexpression on PASMCM migration and proliferation. (A) Representative immunoblot image shows AQP1 and smooth muscle–specific  $\alpha$ -actin (actin) protein levels in cells infected with adenovirus-containing green fluorescent protein (GFP) and AdAQP1 (AQP1). Bar graph showing the mean  $\pm$  SEM values for AQP1 protein expression in GFP- and AQP1-infected cells ( $n = 4$  each). (B) Immunoblot image shows AQP1 surface biotinylation in GFP- and AQP1-infected cells. Bar graph showing mean  $\pm$  SEM values for AQP1 surface biotinylation in GFP- and AQP1-infected cells ( $n = 4$  each). (C) Cellular localization for GFP and AQP1 in infected cells. Confocal images for protein of interest (green) or membrane (red) and merged images in PASMCMs infected with GFP or AQP1. Right panels show Z-stack images for each cell. Images are representative of three cells per experiment for each condition and three separate experiments. (D) Bar graph showing percent migration (mean  $\pm$  SEM) in PASMCMs infected with GFP ( $n = 13$ ) and AQP1 ( $n = 4$ ). (E) Bar graph showing proliferation (mean  $\pm$  SEM) of GFP- and AQP1-infected cells ( $n = 6$  each). \*Significant difference from GFP ( $P < 0.05$ ).

#### Effects of EF-Hand Mutation on PASMCM Migration and Proliferation

Because the C-terminal of AQP1 appeared to play an important role in PASMCM migration and proliferation and because a putative EF-hand motif is located in the

C-terminal tail, we next tested whether mutation of the EF-hand motif would alter AQP1-induced migration and proliferation. First, we confirmed that protein expression for AQP1 with the EF-hand mutation was similar to wild-type

AQP1 by measuring total protein and surface biotinylation (Figures 6A and 6B). Immunoblots showed that infection with AdAQP1-HA or AdAQP1M-HA results in substantial protein and membrane expression of HA-tagged AQP1. The

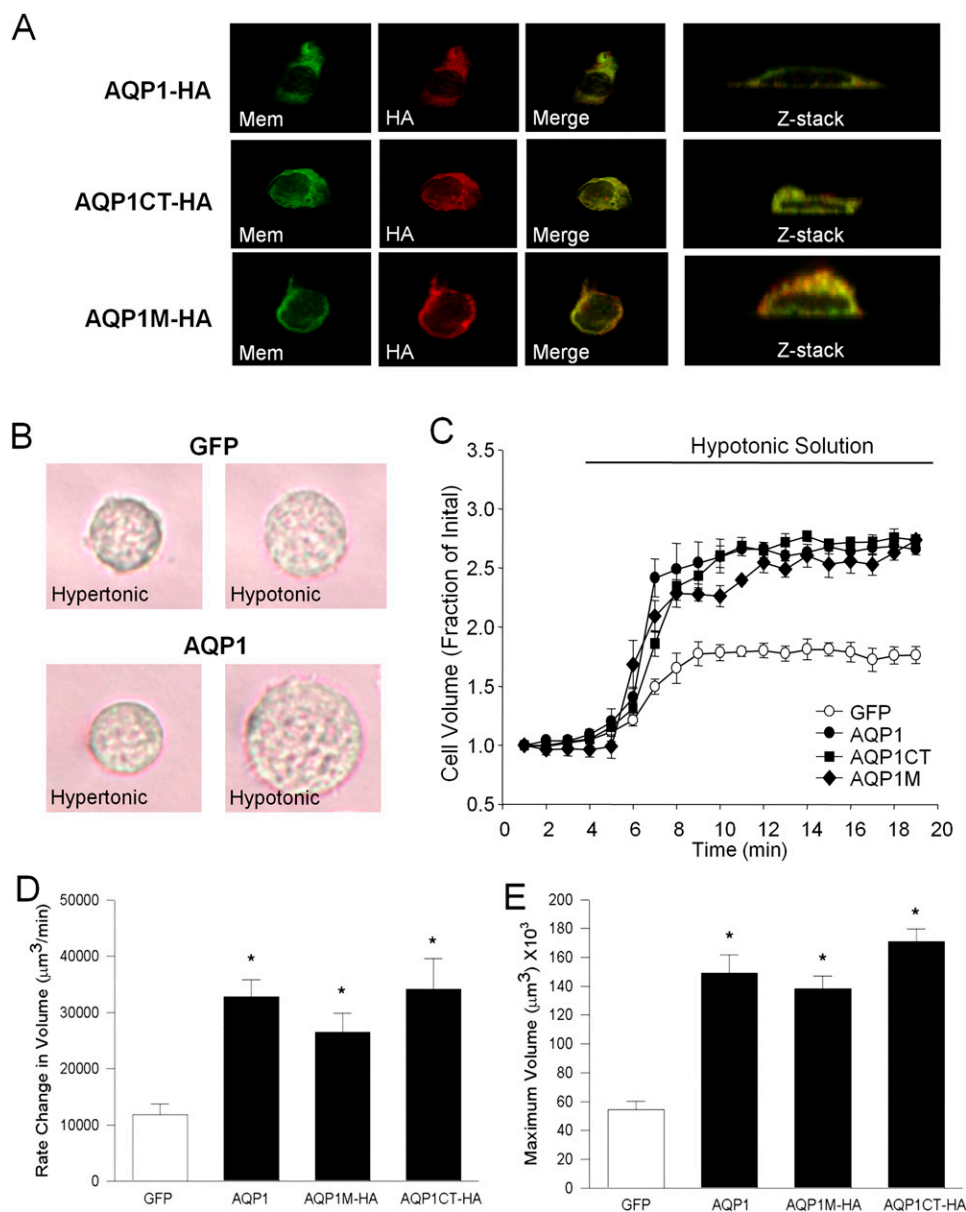


**Figure 3.** (A) Representative confocal images demonstrating cellular localization in PSMCs for hemagglutinin (HA)-tagged AQP1 (AQP1-HA), HA-tagged AQP1 with C-terminal deletion (AQP1CT-HA), and HA-tagged AQP1 with EF-hand mutation (AQP1M-HA). Confocal images are shown for protein of interest (*red*), membrane (*green*), and merged images. *Right panels* show Z-stack for each cell. Images are representative of three cells per experiment for each condition and three separate experiments. (B) Representative images show trypsinized PSMCs infected with AdGFP or AdAQP1 are perfused with hypertonic or hypotonic HEPES-buffered solution. (C) Cell volume increases with expression of wild-type AQP1, AQP1 C-terminal deleted mutant, and AQP1 EF-hand mutant. Bar graphs show rate of volume change (mean  $\pm$  SEM) (D) and maximum volume change (mean  $\pm$  SEM) (E) for PSMCs infected with AdGFP, AdAQP1, AdAQP1CT-HA, and AdAQP1M-HA ( $n = 3$  each). \*Significant difference from AdGFP ( $P < 0.05$ ).

mutated AQP1 appears to migrate slightly faster than wild-type AQP1, and the total level of expression was lower than wild-type AQP1. Nonetheless, infection with AdAQP1M-HA had no effect on cell adherence ( $341 \pm 64$  cells [ $n = 4$ ] vs.  $313 \pm 46$  cells for AdGFP [ $n = 13$ ]) but significantly increased PSMC migration and proliferation (Figures 6C and 6D).

### Discussion

In this study, we demonstrated that modulating the expression of AQP1 altered the migratory and proliferative capacity of PSMCs. Our studies also revealed that the C-terminal tail of AQP1 was critically important for AQP1-mediated migration and proliferation, whereas neither the

putative EF-hand motif in the cytoplasmic tail nor water transport of the channel appear to be involved in these responses.

That knockdown of AQP1 in PSMCs had no effect on basal (unstimulated) rates of migration but completely prevented the hypoxia-induced increase in migration is consistent with our previous study (10) and with evidence from other labs showing

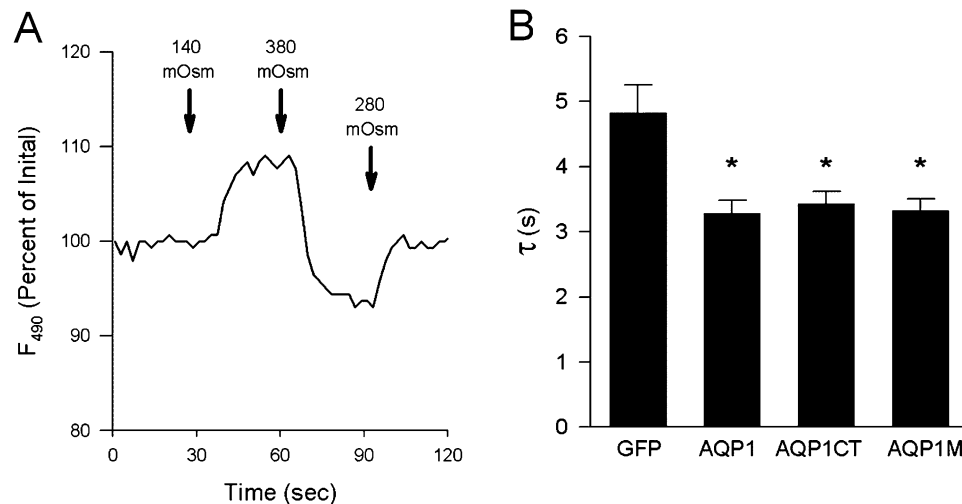


**Figure 4.** Water permeability in PASMCs infected with wild-type and mutated AQP1. (A) Representative trace showing the effect of changes in perfusate osmotic pressure on fluorescence measured in an adherent, calcein-loaded PASMC. Data are expressed as percent of the initial fluorescence at time 0. (B) Bar graph showing mean  $\pm$  SEM values for the time constant of decay ( $\tau$ ) of calcein fluorescence (quenching) when perfusate was switched from 140 to 380 mOsm in cells infected with AdGFP (GFP), AdAQP1-HA (AQP1), AdAQP1CT-HA (AQPCT), or AdAQP1M-HA (AQP1M) ( $n = 4$  each). \*Significant difference from GFP ( $P < 0.05$ ).

that AQP1 was required for stimulated, but not basal, migration in proximal tubule (22) and endothelial cells (12). Similarly, melanoma cells that expressed high levels of AQP1 had increased metastatic potential and local infiltration (15), further supporting a role for AQP1 in enhanced migratory capacity. Even though the protein is abundantly expressed at baseline, our results suggest that migration in unstimulated cells is likely governed by a different mechanism and that AQP1 only appears to contribute under hypoxic conditions.

In contrast to the lack of effect of AQP1 depletion on unstimulated migration, we found that knockdown of AQP1 markedly decreased proliferation of PASMCs under basal conditions. Moreover, loss of AQP1 prevented the increase in PASMC proliferation induced by hypoxia, a well-known stimulus for inducing cell growth, not only in PASMCs (23, 24) but also in neural stem cells (25) and endothelial cells (26). Our results are in line with studies in hepatic endothelial cells derived from AQP1 knockout mice, which showed decreased proliferation after bile duct ligation (27), although proliferation was found to be independent of AQP1 in control hepatic (27) and aortic endothelial (12) and renal epithelial (22) cells. Thus, our loss-of-function experiments demonstrate that AQP1 is an important regulator of migration and proliferation of

PASMCs and that the requirement for AQP1 in these responses may be cell-type specific.

Because we previously found that hypoxia-induced migration of PASMCs was associated with increased AQP1 protein expression (10), we next determined the effect of mimicking hypoxic conditions by overexpressing AQP1 via adenovirus. The 3-fold increase in AQP1 protein expression achieved with viral infection was similar to that observed in response to hypoxia in this cell type (10). The expressed AQP1 protein colocalized with and inserted into the membrane irrespective of whether the protein expressed an HA tag, indicative of proper trafficking of the expressed proteins. Moreover, PASMCs in which AQP1 was expressed exhibited significantly faster increases in volume when subjected to hypotonic challenge, demonstrating proper function of the protein as a water transporter. However, because the methods used to measure cell swelling prevented rapid changes in perfusate and thus resulted in changes in volume that required several minutes to stabilize, it is possible that the changes in cell volume observed using the visual swelling assay were not due solely to water transport via AQP1, which occurs within seconds. Thus, we also used the method of calcein self-quenching (21) to estimate AQP1-mediated water transport, which confirmed the conclusions drawn from the

volume assays. The enhanced PASMC migration and proliferation observed when AQP1 expression was increased were similar in magnitude to those induced by exposure to hypoxia and are consistent with experiments showing that elevating AQP1 expression in fibroblasts was associated with increased cell numbers (28), although in that study cell proliferation was not directly measured. These gain-of-function experiments not only confirm a role for AQP1 in regulating PASMC proliferation but also suggest that an elevation in AQP1 levels alone is sufficient to induce PASMC migration and proliferation absent other components of hypoxic exposure.

The mechanism by which AQP1 might facilitate cell migration or proliferation has been suggested to be due to increased local water transport in lamellipodia (11, 12, 22). However, AQP1 was uniformly distributed in our cells, even under hypoxic conditions (*see* Figure E2 in the online supplement), suggesting that mechanisms other than localized water transport may be important in PASMCs. To begin to dissect the mechanism by which AQP1 facilitates migration and proliferation in our cells, deletion and mutation experiments were performed to identify which parts of the AQP1 protein were required for these processes. The C-terminal of AQP1, located within the cytoplasm and containing potential regulatory sites such as putative EF-hand

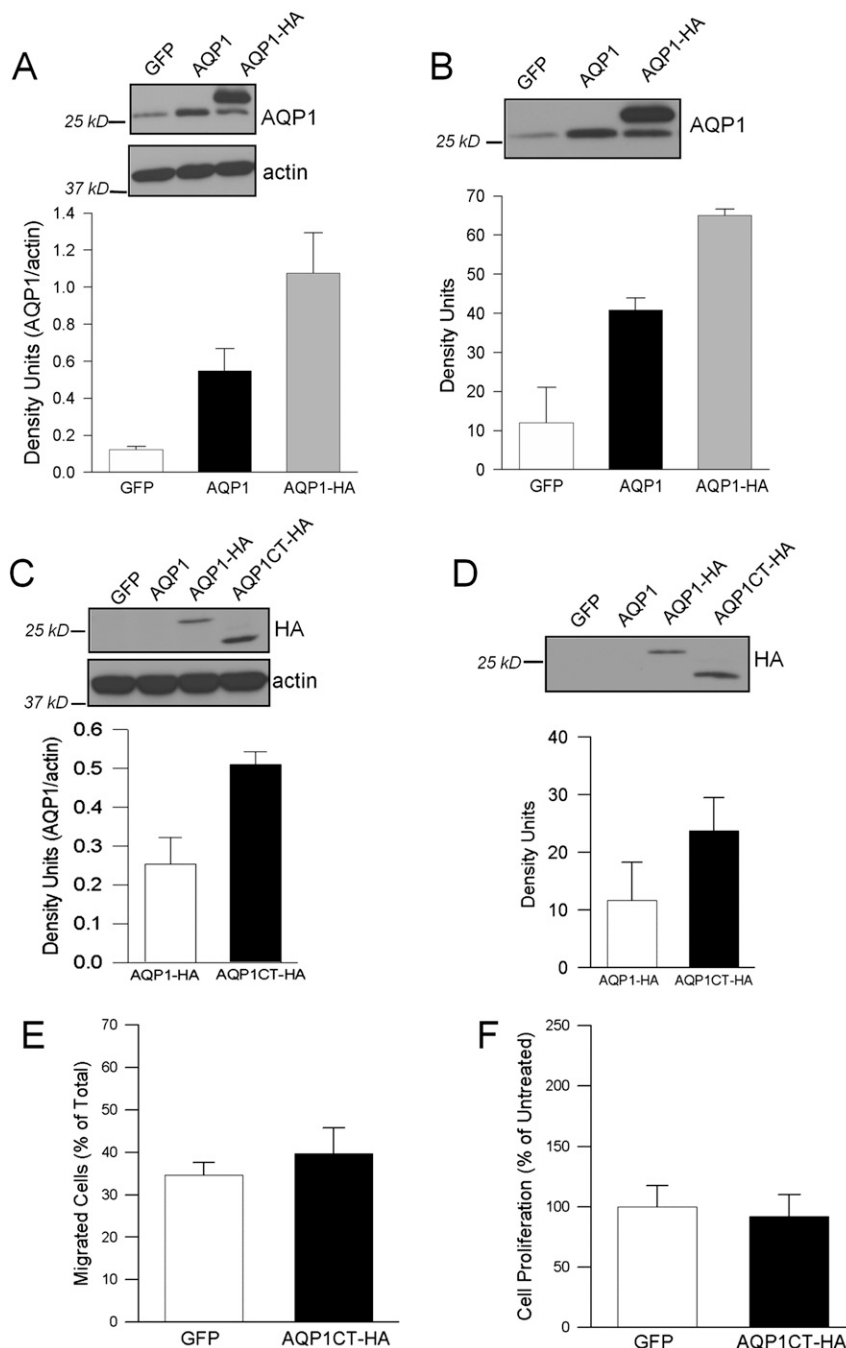


**Figure 5.** Effects of AQP1 with C-terminal deletion on PASC migration and proliferation. (A) Representative immunoblot image shows membrane probed with anti-AQP1 and anti-smooth muscle-specific  $\alpha$ -actin (actin) using protein from cells infected with AdGFP (GFP), AdAQP1 (AQP1), and AdAQP1-HA (AQP1-HA). Bar graph shows mean  $\pm$  SEM values for AQP1 protein expression ( $n = 4$  each). (B) Immunoblot image showing AQP1 surface biotinylation in AdGFP-, AdAQP1-, and AdAQP1-HA-infected cells. Bar graph shows mean  $\pm$  SEM values for AQP1 surface biotinylation in AdGFP-, AdAQP1-, and AdAQP1-HA-infected cells ( $n = 4$  each). (C) Immunoblot image showing the amount of HA-tagged and actin protein in cells infected with AdGFP, AdAQP1, AdAQP1-HA, and AdAQP1CT-HA. Membrane was probed with anti-HA followed by anti-actin. Bar graph shows mean  $\pm$  SEM values for density units of AdAQP1-HA and AdAQP1CT-HA normalized to actin ( $n = 4$  each). (D) Immunoblot image showing the amount of surface biotinylation of HA-tagged protein in cells infected with AdGFP, AdAQP1, AdAQP1-HA, and AdAQP1CT-HA. Bar graph shows mean  $\pm$  SEM density units of AdAQP1-HA and AdAQP1CT-HA surface biotinylation (HA-tagged;  $n = 4$  each). (E) Bar graph showing percent migration (mean  $\pm$  SEM) in PASCs infected with AdGFP ( $n = 13$ ) and AdAQP1CT-HA ( $n = 5$ ). (F) Bar graph showing the proliferation (mean  $\pm$  SEM) in PASCs infected with AdGFP and AdAQP1CT-HA ( $n = 4$  each).

and cyclic guanosine monophosphate binding motifs (19), provided an attractive starting point. A truncated version of

AQP1, lacking the C-terminal cytoplasmic tail, still localized correctly and inserted into the membrane to a similar extent as

full-length AQP1 and appeared to be expressed at even greater levels than the wild-type AQP1, indicating that the



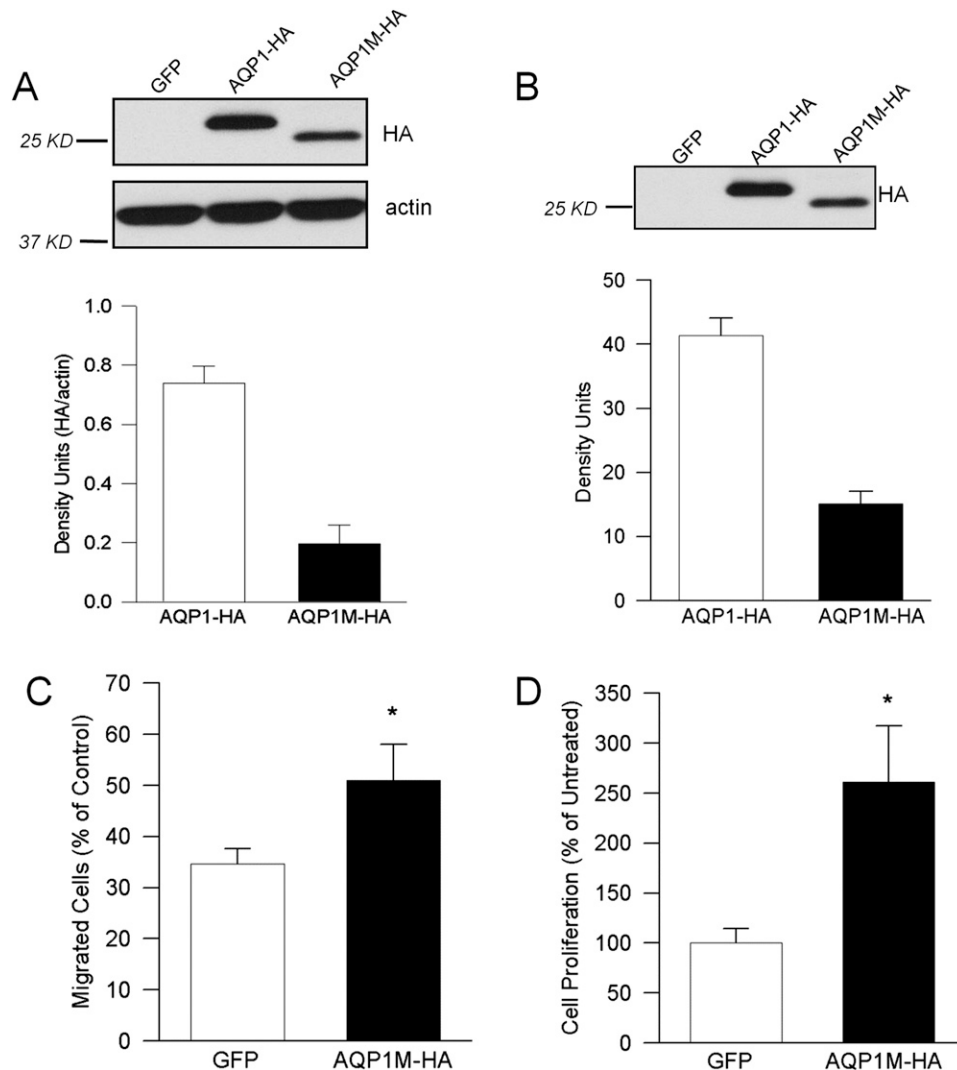


**Figure 6.** Effects of AQP1 with EF-hand mutation on PASMCM migration and proliferation. (A) Immunoblot image showing the amount of HA-tagged and smooth muscle-specific  $\alpha$ -actin (actin) protein in cells infected with AdGFP (GFP), AdAQP1-HA (AQP1-HA), and AdAQP1M-HA (AQP1M-HA). Bar graph shows mean  $\pm$  SEM density units (normalized to actin) of HA-tagged protein in PASMCMs infected with AdAQP1-HA and AdAQP1M-HA ( $n = 4$  each). (B) Immunoblot image shows amount of biotinylated HA-tagged protein in cells infected with AdGFP, AdAQP1-HA, and AdAQP1M-HA. Bar graph shows mean  $\pm$  SEM density units of surface biotinylated HA-tagged proteins ( $n = 4$  each). (C) Bar graph showing the percent migration (mean  $\pm$  SEM) in PASMCMs infected with AdGFP ( $n = 13$ ) and AdAQP1M-HA ( $n = 4$ ). (D) Bar graph showing proliferation (mean  $\pm$  SEM) in PASMCMs infected with AdGFP and AdAQP1M-HA ( $n = 4$  each). \*Significant difference from AdGFP ( $P < 0.05$ ).

C-terminal was not required for proper protein targeting to the membrane. Previous reports showed that although the C-terminal tail of AQP1 may be involved in modulating AQP1 activity (19), it was not necessarily required for basal water transport (29). Our results appear to verify this notion. We observed similar increases in cell volume and reductions in time constant for calcein quenching with full-length and truncated AQP1. Contrary to the enhanced migration and proliferation observed with expression of wild-type AQP1, expression of AQP1

lacking the C-terminal tail had no effect on either cell function, indicating a primary role for the C-terminal cytoplasmic tail. Our results suggest that the possible mechanisms by which AQP1 mediates PASMCM migration and proliferation include association of factors or proteins with the C-terminal of AQP1 but appear to rule out a role for AQP1-facilitated transmembrane water transport.

We next focused on the putative calcium binding site, or EF-hand motif, in the C-terminal of AQP1 (19).

Accumulating data show that calcium plays an important role in migration and proliferation in a variety of cell types, including PASMCMs (2, 10, 30–33), via mechanisms including regulation of focal adhesion turnover (33–35), activation of  $Ca^{2+}$ /calmodulin kinase (36), actin-binding proteins (35), and myosin II (37), leading to force generation necessary to move the cell and activation of gelsolin to promote filament severing and depolymerization (35, 37). Thus, we hypothesized that calcium might also be required for AQP1-mediated migration

and proliferation via binding to the EF-hand motif in the C-terminal of AQP1. The EF-hand mutant localized properly and facilitated water transport similar to the wild-type protein. The expression levels of the EF-hand mutant were lower than those achieved with similar levels of wild-type AQP1, perhaps reflecting Ca<sup>2+</sup>-dependent regulation of protein expression. This notion is consistent with our previous work demonstrating that induction of AQP1 protein by hypoxia required calcium influx (10). Despite lower protein levels, expression of the EF-hand mutant increased PASMCM migration and proliferation.

In summary, the gain-of-function and loss-of-function experiments performed in this study demonstrate a clear role for AQP1 in mediating PASMCM migration and proliferation. The exact mechanism by which AQP1 mediates these responses is incompletely understood; however, experiments using AQP1 proteins in which the C-terminal was deleted or the EF-hand was mutated revealed that although the C-terminal cytoplasmic tail of AQP1 is required, the increased migration and proliferation induced by AQP1 was independent of AQP1 function as water channel or an intact C-terminal EF-hand motif. Recent evidence suggests that AQP1

may play a role in migration of human melanoma and endothelial cells through interaction with Lin-7 and regulation of  $\beta$ -catenin levels (16); further experiments are required to determine if this pathway is also responsible for AQP1-dependent migration and proliferation in our cells. Nonetheless, our findings provide new insights into the function of AQP1 in PASMCMs and suggest a potential role for AQP1 in mediating pulmonary vascular remodeling during the development of hypoxic pulmonary hypertension. ■

**Author disclosures** are available with the text of this article at [www.atsjournals.org](http://www.atsjournals.org).

## References

1. Stenmark KR, Fagan KA, Frid MG. Hypoxia-induced pulmonary vascular remodeling: cellular and molecular mechanisms. *Circ Res* 2006;99:675–691.
2. Shimoda L, Laurie S. Vascular remodeling in pulmonary hypertension. *J Mol Med* 2013;91:297–309.
3. Rabinovitch M, Gamble W, Nadas AS, Miettinen OS, Reid L. Rat pulmonary circulation after chronic hypoxia: hemodynamic and structural features. *Am J Physiol* 1979;236:H818–H827.
4. Yu AY, Shimoda LA, Iyer NV, Huso DL, Sun X, McWilliams R, Beaty T, Sham JS, Wiener CM, Sylvester JT, et al. Impaired physiological responses to chronic hypoxia in mice partially deficient for hypoxia-inducible factor 1 $\alpha$ . *J Clin Invest* 1999;103:691–696.
5. Frank DB, Abtahi A, Yamaguchi DJ, Manning S, Shyr Y, Pozzi A, Baldwin HS, Johnson JE, de Caestecker MP. Bone morphogenetic protein 4 promotes pulmonary vascular remodeling in hypoxic pulmonary hypertension. *Circ Res* 2005;97:496–504.
6. White TA, Witt TA, Pan S, Mueske CS, Kleppe LS, Holroyd EW, Champion HC, Simari RD. Tissue factor pathway inhibitor overexpression inhibits hypoxia-induced pulmonary hypertension. *Am J Respir Cell Mol Biol* 2010;43:35–45.
7. Girgis RE, Mozammel S, Champion HC, Li D, Peng X, Shimoda L, Tudor RM, Johns RA, Hassoun PM. Regression of chronic hypoxic pulmonary hypertension by simvastatin. *Am J Physiol Lung Cell Mol Physiol* 2007;292:L1105–L1110.
8. Pietra GG, Capron F, Stewart S, Leone O, Humbert M, Robbins IM, Reid LM, Tudor RM. Pathologic assessment of vasculopathies in pulmonary hypertension. *J Am Coll Cardiol* 2004;43:25S–32S.
9. Ishibashi K, Hara S, Kondo S. Aquaporin water channels in mammals. *Clin Exp Nephrol* 2009;13:107–117.
10. Leggett K, Maylor J, Udem C, Lai N, Lu W, Schweitzer K, King LS, Myers AC, Sylvester JT, Sidhaye V, et al. Hypoxia-induced migration in pulmonary arterial smooth muscle cells requires calcium-dependent upregulation of aquaporin 1. *Am J Physiol Lung Cell Mol Physiol* 2012;303:L343–L353.
11. Papadopoulos MC, Saadoun S, Verkman AS. Aquaporins and cell migration. *Pflugers Arch* 2008;456:693–700.
12. Saadoun S, Papadopoulos MC, Hara-Chikuma M, Verkman AS. Impairment of angiogenesis and cell migration by targeted aquaporin-1 gene disruption. *Nature* 2005;434:786–792.
13. Agre P, Preston GM, Smith BL, Jung JS, Raina S, Moon C, Guggino WB, Nielsen S. Aquaporin CHIP: the archetypal molecular water channel. *Am J Physiol* 1993;265:F463–F476.
14. Hayashi S, Takahashi N, Kurata N, Yamaguchi A, Matsui H, Kato S, Takeuchi K. Involvement of aquaporin-1 in gastric epithelial cell migration during wound repair. *Biochem Biophys Res Commun* 2009;386:483–487.
15. Hu J, Verkman AS. Increased migration and metastatic potential of tumor cells expressing aquaporin water channels. *FASEB J* 2006;20:1892–1894.
16. Monzani E, Bazzotti R, Perego C, La Porta CA. AQP1 is not only a water channel: it contributes to cell migration through Lin7/ $\beta$ -catenin. *PLoS ONE* 2009;4:e6167.
17. Gonen T, Walz T. The structure of aquaporins. *Q Rev Biophys* 2006;39:361–396.
18. Preston GM, Carroll TP, Guggino WB, Agre P. Appearance of water channels in *Xenopus* oocytes expressing red cell CHIP28 protein. *Science* 1992;256:385–387.
19. Fotiadis D, Suda K, Tittmann P, Jenö P, Philippsen A, Müller DJ, Gross H, Engel A. Identification and structure of a putative Ca<sup>2+</sup>-binding domain at the C terminus of AQP1. *J Mol Biol* 2002;318:1381–1394.
20. Li L, Zhang H, Ma T, Verkman AS. Very high aquaporin-1 facilitated water permeability in mouse gallbladder. *Am J Physiol Gastrointest Liver Physiol* 2009;296:G816–G822.
21. Solenov E, Watanabe H, Manley GT, Verkman AS. Sevenfold-reduced osmotic water permeability in primary astrocyte cultures from AQP-4-deficient mice, measured by a fluorescence quenching method. *Am J Physiol Cell Physiol* 2004;286:C426–C432.
22. Hara-Chikuma M, Verkman AS. Aquaporin-1 facilitates epithelial cell migration in kidney proximal tubule. *J Am Soc Nephrol* 2006;17:39–45.
23. Schultz K, Fanburg BL, Beasley D. Hypoxia and hypoxia-inducible factor-1 $\alpha$  promote growth factor-induced proliferation of human vascular smooth muscle cells. *Am J Physiol Heart Circ Physiol* 2006;290:H2528–H2534.
24. Yu L, Hales CA. Silencing of sodium-hydrogen exchanger 1 attenuates the proliferation, hypertrophy, and migration of pulmonary artery smooth muscle cells via E2F1. *Am J Respir Cell Mol Biol* 2011;45:923–930.
25. Santilli G, Lamorte G, Carlessi L, Ferrari D, Rota Nodari L, Binda E, Delia D, Vescevi AL, De Filippis L. Mild hypoxia enhances proliferation and multipotency of human neural stem cells. *PLoS ONE* 2010;5:e8575.
26. Meininger CJ, Schelling ME, Granger HJ. Adenosine and hypoxia stimulate proliferation and migration of endothelial cells. *Am J Physiol* 1988;255:H554–H562.
27. Huebert RC, Jagavelu K, Hendrickson HI, Vasdev MM, Arab JP, Splinter PL, Trussoni CE, Larusso NF, Shah VH. Aquaporin-1 promotes angiogenesis, fibrosis, and portal hypertension through mechanisms dependent on osmotically sensitive microRNAs. *Am J Pathol* 2011;179:1851–1860.
28. Hoque MO, Soria JC, Woo J, Lee T, Lee J, Jang SJ, Upadhyay S, Trink B, Monitto C, Desmazes C, et al. Aquaporin 1 is overexpressed in lung cancer and stimulates NIH-3T3 cell proliferation and anchorage-independent growth. *Am J Pathol* 2006;168:1345–1353.

29. Saparov SM, Kozono D, Rothe U, Agre P, Pohl P. Water and ion permeation of aquaporin-1 in planar lipid bilayers: major differences in structural determinants and stoichiometry. *J Biol Chem* 2001;276:31515–31520.
30. Shimoda LA, Udem C. Interactions between calcium and reactive oxygen species in pulmonary arterial smooth muscle responses to hypoxia. *Respir Physiol Neurobiol* 2010;174:221–229.
31. Tauzin S, Chaigne-Delalande B, Selva E, Khadra N, Daburon S, Contin-Bordes C, Blanco P, Le Seyec J, Ducret T, Counillon L, *et al*. The naturally processed CD95L elicits a c-yes/calcium/PI3K-driven cell migration pathway. *PLoS Biol* 2011;9:e1001090.
32. Hatzia Apostolou M, Koukos G, Polytaichou C, Kottakis F, Serebrennikova O, Kuliopulos A, Tsihchlis PN. Tumor progression locus 2 mediates signal-induced increases in cytoplasmic calcium and cell migration. *Sci Signal* 2011;4:ra55.
33. Howe AK. Cross-talk between calcium and protein kinase A in the regulation of cell migration. *Curr Opin Cell Biol* 2011;23:554–561.
34. Millon-Frémillon A, Brunner M, Abed N, Collomb E, Ribba AS, Block MR, Albigès-Rizo C, Bouvard D. Calcium and calmodulin-dependent serine/threonine protein kinase type II (CaMKII)-mediated intramolecular opening of integrin cytoplasmic domain-associated protein-1 (ICAP-1 $\alpha$ ) negatively regulates  $\beta$ 1 integrins. *J Biol Chem* 2013;288:20248–20260.
35. Khurana S, George SP. Regulation of cell structure and function by actin-binding proteins: villin's perspective. *FEBS Lett* 2008;582: 2128–2139.
36. Pauly RR, Bilato C, Sollott SJ, Monticone R, Kelly PT, Lakatta EG, Crow MT. Role of calcium/calmodulin-dependent protein kinase II in the regulation of vascular smooth muscle cell migration. *Circulation* 1995;91:1107–1115.
37. Gerthoffer WT. Mechanisms of vascular smooth muscle cell migration. *Circ Res* 2007;100:607–621.